Optoacoustic detection of early therapy-induced tumor cell death using a targeted imaging agent

Bangwen Xie[1], Michal R. Tomaszewski[1], André A. Neves[1], Susana Ros[1], De-En Hu[1], Sarah McGuire[1], Stefanie R. Mullins[2], David Tice[3], Richard C.A. Sainson[2,4], Sarah E. Bohndiek[1], Robert W. Wilkinson[2], Kevin M. Brindle[1]

1 Cancer Research UK Cambridge Institute, Li Ka Shing Centre, University of Cambridge, Robinson Way, Cambridge CB2 0RE, UK

2 MedImmune Limited, Granta Park, Cambridge, CB21 6GH, UK

3 MedImmune LLC, 1 MedImmune Way, Gaithersburg, MD 20878, USA

4 Current address: Kymab Ltd, Cambridge, CB22 3AT UK

Running title: Optoacoustic imaging of tumor cell death

Key words: tumor, cell death, TRAIL, optoacoustic imaging

Grant support: The work was supported by a Cancer Research UK Programme grant (17242) and a Project grant from MedImmune to KMB and by the CRUK-EPSRC Imaging Centre in Cambridge and Manchester (16465).

Corresponding author: Prof. Kevin M. Brindle, Cancer Research UK Cambridge Institute, Li Ka Shing Centre, Robinson Way, Cambridge, CB2 0RE, United Kingdom, Phone: 01223 769647, Fax: 01223 766002

e-mail: kmb1001@cam.ac.uk

Competing financial interests: This work was funded, in part, by MedImmune who have a financial interest in the drug used here and in drugs of this type.

Statement of translational relevance:

Tumors of the same type can show markedly different responses to the same treatment. The development of new treatments and their deployment in the clinic would benefit, therefore, from the introduction of imaging methods that allow an early assessment of treatment response in individual patients, allowing rapid selection of the most effective treatment for a specific patient. Multispectral optoacoustic tomography (MSOT) is a clinically applicable, real-time imaging modality that can generate relatively high-resolution cross-sectional images at depth. We show here that when used with a near infra-red (NIR) fluorophore-labelled probe that binds to apoptotic and necrotic cells MSOT can be used to image tumor cell death within an entire tumor volume. The technique can be used to characterize the heterogeneous response of a tumor to treatment and to determine the most effective therapy at an early stage following the start of treatment.

Abstract

Purpose: The development of new treatments and their deployment in the clinic may be assisted by imaging methods that allow an early assessment of treatment response in individual patients. The C2A domain of Synaptotagmin-I (C2Am), which binds to the phosphatidylserine (PS) exposed by apoptotic and necrotic cells, has been developed as an imaging probe for detecting cell death. Multispectral optoacoustic tomography (MSOT) is a real-time and clinically applicable imaging modality that was used here with a near infrared (NIR) fluorophore-labeled C2Am to image tumor cell death in mice treated with a TNF-related apoptosis-inducing ligand receptor 2 (TRAILR2) agonist and with 5-fluorouracil (5-FU).

Experimental design: C2Am was labeled with a near infrared (NIR) fluorophore and injected intravenously into mice bearing human colorectal TRAIL-sensitive Colo205 and TRAIL-resistant HT-29 xenografts that had been treated with a potent agonist of TRAILR2 and in Colo205 tumors treated with 5-FU.

Results: Three dimensional MSOT images of probe distribution showed development of tumor contrast within 3 h of probe administration and a signal-to-background ratio in regions containing dead cells of >10 after 24 h. A site-directed mutant of C2Am that is inactive in PS binding showed negligible binding. Tumor retention of the active probe was strongly correlated (R^2=0.97, P value<0.01) with a marker of apoptotic cell death measured in histological sections obtained post mortem.

Conclusions: The rapid development of relatively high levels of contrast suggests that NIR fluorophore-labeled C2Am could be a useful optoacoustic imaging probe for detecting early therapy-induced tumor cell death in the clinic.

Introduction

DNA sequencing of tumor biopsies or of circulating tumor DNA (ctDNA), and detection of early treatment response through increases in the levels of ctDNA, are expected to play an increasingly important role in selecting treatment for individual patients (1,2). However, tumor heterogeneity remains an obstacle for both approaches. Biopsies may not detect all clones present within a tumor and the presence of residual treatment-resistant clones may not be reflected in the levels of ctDNA released following treatment. Imaging methods that can detect treatment response throughout the entire tumor volume are likely, therefore, to play an important role in treatment selection (3).

Tumor cell death represents a generic downstream marker of treatment response and consequently there has been considerable interest in developing imaging methods and agents to detect tumor cell death *in vivo* (4). We have developed a targeted imaging agent based on the C2A domain of Synaptotagmin-I, which binds with nanomolar affinity to the phosphatidylserine (PS) exposed on the plasma membrane of dying cells (5). The protein was used initially as a glutathione-S-transferase (GST) fusion protein, where imaging labels were attached to lysine residues, and used to detect tumor cell death using magnetic resonance and radionuclide imaging (6-9). Subsequently, we developed a much smaller derivative of C2A (16 kDa) based on the isolated C2A domain (C2Am), in which we introduced a unique cysteine residue distant from the PS binding site. This allowed site-specific attachment of imaging labels, without affecting binding affinity, and the production of a chemically homogeneous preparation of the agent. The smaller size allows for relatively rapid renal clearance, the production of a homogeneous agent rules out the possibility of labeled material that does not bind PS, or shows only weak binding,

and the removal of the GST tag, by lowering potential immunogenicity, increases clinical translatability. C2Am, when labeled with a fluorophore, showed better specificity for binding to dead cells than a similarly labeled Annexin V derivative (5). Fluorescently labeled Annexin V is widely used to detect cell death *in vitro* and, in radionuclide-labeled form, has also translated to the clinic. However, clinical use of this agent was limited by poor specificity and relatively high levels of background binding (10).

The relatively high sensitivity, minimal tissue absorption and low cost of near infrared (NIR) fluorescence imaging have made this a widely used technique for non-invasive imaging in small animals (11) and increasingly in the clinic (12). However, image depth and resolution are limited by scattering, with depths of 1-2 cm and resolutions of 1-2 mm (13). Optoacoustic imaging can give three-dimensional (3D) tomographic images and can generate relatively high-resolution images at depths of a few centimeters. In this technique NIR radiation is administered in the form of nanosecond laser pulses. Absorption by chromophores in endogenous materials, such as oxy- and deoxyhemoglobin and melanin, or in contrast agents introduced exogenously, results in thermoelastic expansion and the production of a pressure wave that can be detected non-invasively using ultrasound transducers. Since pressure waves are relatively low frequency they are scattered much less than light or NIR radiation and so can be used to generate much higher resolution images. Detectors operating around 5 MHz enable penetration depths of several centimeters with resolutions between 100–400 μm, while detectors operating in the 10–100 MHz frequency range penetrate 1–10 mm with resolutions in the tens of micrometres (14). In multispectral optoacoustic tomography (MSOT) measurements are made at several NIR wavelengths in less than a second, which enables real-time imaging of

individual chromophores within entire tumor volumes. With the introduction of a hand held device, bed-fitted devices and the development of real-time three-dimensional optoacoustic tomography (14,15), clinical applications of MSOT have started to emerge, including screening of dense breasts for the presence of tumors (16,17), monitoring the metastatic status of sentinel lymph nodes in melanoma patients (18) and assessment of inflammatory disease (19).

Tumor necrosis factor (TNF)-related apoptosis-inducing ligand receptor 2 (TRAILR2) is a death receptor upregulated in a wide range of human tumors (20-22), which upon ligation triggers apoptosis through activation of a caspase cascade. MEDI3039 is a multivalent TRAILR2 agonist that can induce cell death in tumor cells at picomolar concentrations (23,24).

We describe here *in vivo* imaging measurements of early tumor responses to MEDI3039, and also 5-FU, using NIR fluorophore-labeled C2Am, using both optical imaging and MSOT. Non-specific probe binding was assessed using a site-directed mutant that is inactive in PS binding (iC2Am) (25). The MSOT signal from C2Am was increased significantly in MEDI3039 and 5-FU-treated Colo205 tumors as early as 3 h post probe injection, whereas there was negligible retention of iC2Am in MEDI3039-treated tumors. Subsequent histological analyses showed that the C2Am signal observed *in vivo* was strongly correlated with immunostaining of dead cells in tumor sections.

Materials and methods

Cell culture. Human colorectal adenocarcinoma Colo205 cells were cultured in RPMI-1640 medium (Life Technologies Ltd., Paisley, UK) and HT-29 in McCoy's 5A (Modified), GlutaMAX™ medium (Life Technologies Ltd.). Both media were

supplemented with 10% fetal bovine serum (FBS; Lonza, Basel Switzerland). The cell lines were purchased from ATCC and both tested negative for mycoplasma by a RNA capture ELISA-based method. Cell lines were cultured in a humidified incubator at 37° C and 5% CO_2. The sensitivities of Colo205 and HT-29 cells to MEDI3039 treatment were assessed by measuring cell viability at 22 h after drug treatment. Briefly, the cells were collected after drug treatment and resuspended to a density of 1 x 10^6 cells/mL in medium. Ten µL cell samples were mixed with ten µL Trypan blue dye solution and cell viability assessed using a cell viability analyzer (Luna™ Automated Cell Counter, Logos Biosystems, France). Cell viability was also assessed in Colo-Dual cells, which expressed luciferase (see below), by the addition of D-luciferin solution (25 µg/µl; SynChem Inc., Elk Grove Village, IL) to a 96-well with 5,000 cells per well. Bioluminescence imaging (BLI) measurements were performed 10 minutes later using an IVIS 200 series camera (PerkinElmer, Waltham, MA) with an F-stop of 1 and open filter. All the samples were prepared in triplicate.

Generation of Colo-Dual cell lines. Cells were transduced with a lentiviral vector in which the EF1 promoter drives transcription of the red fluorescent protein, mStrawberry, and firefly luciferase (26). The mStrawberry coding sequence is separated from the luciferase coding sequences by an E2A sequence (EF1-L-S), which results in similar levels of expression of mStrawberry and luciferase. Lentiviruses were produced by co-transfecting HEK 293T cells with the EF1-L-S plasmid and packaging plasmids. Supernatants containing lentiviruses were collected 72 h after transfection, mixed with polybrene (8 µg/ml) and used to infect Colo205 cells. After 72 h cells displaying similar levels of red fluorescence were sorted, using a BD FACSAria cell sorter (BD Biosciences, Rockville, MD).

Conjugates of C2Am and iC2Am. Conjugates of C2Am and iC2Am with VivoTag®-S 750-MAL (excitation wavelength: 750±5nm; emission wavelength: 775±5nm, PerkinElmer, Waltham, MA) and iC2Am with IRDye® 680RD (excitation wavelength: 672nm; emission wavelength: 694nm, LI-COR Biosciences, Lincoln, NE) were prepared as described previously (5). This conjugation protocol has been shown previously to produce conjugates of C2Am and iC2Am that were fully modified, yielding a single molecular species on electrospray ionization mass spectrometry (5,25). The optical absorption spectrum of 1 μM C2Am-750 in phosphate-buffered saline (PBS) was measured using a PHERAStar FS spectrometer (BMG LABTECH, Bucks, UK).

Flow Cytometry. Following treatment with 1 pM MEDI3039 for 22 h, Colo205 and HT-29 cells were resuspended in 100 μL of pre-cooled HEPES-buffered saline (10 mM HEPES, 150 mM NaCl, 2 mM $CaCl_2$, pH 7.4) with 1% FBS. The cell suspensions were incubated with a 1:1 mixture of C2Am-750 and iC2Am-680 at a concentration of 300 nM, and SYTOX Green (Invitrogen; 50 nM) for 20 min at 37 °C, and then washed twice and kept briefly on ice before being analyzed using an LSR II cytometer (BD Biosciences). For blocking experiments, the cell suspensions were first incubated with an excess of unlabeled C2Am (30 μM) for 30 min before the addition of labeled C2Am and iC2Am. Data were analyzed using FlowJo software. MEDI3039 was supplied as a stock solution of 10 mg/mL in PBS.

Confocal microscopy. Colo-Dual cells were cultured in a glass bottomed culture dish (MatTek Crop., Ashland, MA) until 80% confluent. Cell death was induced by

incubation of the cells with 10 pM MEDI3039 for 5 h. The cells were then incubated in 200 µL of RPMI-1640 medium with a 1:1 mixture of C2Am-750 and iC2Am-680 at a concentration of 500 nM for 20 min at 37°C. The cells were then washed twice gently with phenol red-free RPMI-1640 medium (Life Technologies Ltd.) and imaged using a Leica TCS SP5 confocal microscope (Leica Microsystems Ltd, Milton Keynes, UK). Intrinsic NADH autofluorescence was measured using an Argon-UV laser, with an excitation wavelength range of 340±30 nm, and an emission bandpass filter of 411 - 491 nm. mStrawberry fluorescence was measured using a HeNe 543 laser, with an excitation peak at 574 nm, and an emission bandpass filter of 560 - 620 nm.

Animal Experiments. Female nude mice at ~20 g (BALB/c *nu/nu*, ~8 weeks old) were acquired from Charles River Laboratories. All surgical and imaging procedures were performed under isoflurane gas anesthesia (3% for induction, 2% for maintenance). Animals were sacrificed by cervical dislocation at the endpoint. All animal experiments were carried out under the authority of project and personal licenses issued by the United Kingdom Home Office under the United Kingdom Animals (Scientific Procedures) Act, 1986, and had been reviewed by the Cancer Research UK, Cambridge Institute Animal Welfare and Ethical Review Body.

Imaging Procedures. For fluorescence imaging two groups of mice (n = 5 each) were implanted with 5 x 10^6 Colo205 cells. Two weeks later one group received a single intravenous (i.v.) injection of 0.4 mg/kg MED3039. Another group, which served as an untreated control, were injected with solvent vehicle (PBS). After 16 h the mice were injected i.v. with a mixture of 0.1 µmole/kg C2Am-750 and 0.1

μmole/kg iC2Am-680 (0.2 mL of a solution containing 10 μM of each probe) and fluorescence images were acquired 0.5 and 3 h later using an IVIS 200 series camera with an F-stop of 2. The wavelengths used for fluorescence imaging were dictated by the available filter sets on the IVIS camera. (i)C2Am-750 was imaged with an excitation bandpass filter of 705 - 780 nm and an emission bandpass filter of 810-885 nm. iC2Am - 680 was imaged with an excitation bandpass filter of 615 - 665 nm and an emission bandpass filter of 695 - 770 nm. A correction factor of 3.98 was applied to signals from C2Am-750, when comparing them with iC2Am-680, due to the differences in fluorescence emission from the two fluorophores. The correction factor was calculated by measuring the fluorescence intensities, using the IVIS camera, of iC2Am-680 and C2Am-750 diluted to a concentration of 2 μM in PBS containing 1% FBS. The average radiant efficiency of iC2Am-680 was then divided by the average radiant efficiency of C2Am-750 to obtain a factor that could be used to correct for the more intense fluorescence of the 680 dye. Similar fluorescence measurements were made in groups of mice (n = 3) implanted with 5×10^6 HT-29 cells. Regions of interest were analyzed using Living Image software (PerkinElmer).

For BLI, two groups of mice (n = 5 each) were implanted with 5×10^6 Colo-Dual cells. After 11 days images were acquired from both groups of animals 10 min after intraperitoneal injection (i.p.) of D-luciferin (150 mg/kg) using the IVIS camera with an F-stop of 1 and an open filter. The treated group was then injected with a single dose of 0.4mg/kg MEDI3039. Untreated animals (n=5) were injected with drug vehicle (PBS) and images were acquired two to three times per week from both groups.

For optoacoustic imaging, a MultiSpectral Optoacoustic Tomography (MSOT) inVision 256-TF small animal imaging system (iThera Medical, Munich, Germany) was used. Briefly, a tunable optical parametric oscillator (OPO) pumped by an Nd:YAG laser provides excitation pulses with a duration of 9 ns at wavelengths from 660 nm to 1300 nm at a repetition rate of 10 Hz with a wavelength tuning speed of 10 ms and a peak pulse energy of 90 mJ at 720 nm. Ten arms of a fiber bundle provide uniform illumination of a ring-shaped light strip of approximately 8 mm width. For ultrasound detection, 256 toroidally focused ultrasound transducers, with a center frequency of 5 MHz (60% bandwidth) and organized in a concave array of 270 degree angular coverage and a radius of curvature of 4 cm, are used (27). Two groups of mice (n=5 each) were implanted with 5 x 10^6 Colo205 cells and two weeks later received a single dose of 0.4 mg/kg MED3039. After 4 h, the mice were injected with either 0.2 µmole/kg of C2Am-750 or iC2Am-750 and imaged. Another group (n=3), that were not treated with MEDI3039, were injected with 0.2 µmole/kg of C2Am-750. For imaging, animals were anesthetized and placed on a heated pad before transferring into a custom-made cling film holder (iThera Medical). A small amount of distilled water was placed between the skin of the mouse and the layer of cling film for ultrasound coupling. The holder was placed in the MSOT scanner in a water bath maintained at a temperature of 36°C. MSOT measurements were performed before and at 3, 5, 7 and 24 h after probe injection, according to a protocol described previously (28). Cross-sectional multispectral image datasets were acquired at different wavelengths in the NIR window (660, 665, 670, 680, 690, 700, 710, 720, 730, 740, 750, 755, 760, 770, 780, 800, 825, 850 and 900 nm) through the entire tumor region in 0.5 mm steps in the z-direction and at a single position where the kidneys were located. Scans at each illumination wavelength took

100 ms to acquire, and 10 averages were used to produce a final image, amounting to 20 s acquisition time per slice. Images were reconstructed using a model-based reconstruction algorithm, after which linear spectral unmixing was applied to each set of multi-wavelength images to resolve the biodistribution of the different tissue chromophores i.e. (i)C2Am-750, oxygenated and deoxygenated hemoglobin. Data were processed and quantified using the ViewMSOT software (iThera Medical). Volumetric quantification was done by comparing the signal-to-background ratio after drawing 3D reconstructed volumes of interest (VOIs) in the tumor area. Briefly, a signal-to-background ratio was calculated from the mean pixel intensity (MPI) of a VOI, drawn in an area where there was maximum signal, divided by the MPI of an adjacent size-matched VOI with low signal intensity. The volume percentage of tumor bound by C2Am-750 was taken as the volume with C2Am-750 signal above a threshold value (VT), where this was defined as the mean intensity of the background signal in the tumor volume before probe injection, divided by the total tumor volume (V). This was compared with CC3 staining, where this was determined in tumor sections taken every 2 – 3 mm through the tumor volume. Corresponding fluorescence imaging measurements were made using an IVIS camera immediately after the MSOT measurements.

Similar fluorescence and MSOT measurements were also made in Colo205 tumor-bearing animals treated with 5-fluorouracil (5-FU). Mice (n = 5) were implanted with 5×10^6 Colo205 cells and then two weeks later fluorescence and MSOT measurements were performed before and 3 h after i.v. injection of 0.2 µmole/kg of C2Am-750. Twenty four hours later the animals received a single intraperitoneal injection (250 mg/kg) of 5-FU and then 24 h after drug treatment the fluorescence

and MSOT measurements were repeated. The mean MSOT voxel intensity in the tumor area was compared before and after 5-FU treatment. For the biodistribution study the tumors and major organs, including kidney, spleen, heart, lung, liver, muscle and blood were excised immediately after completion of the *in vivo* imaging, weighed and then their fluorescence imaged using the IVIS-200 camera.

Histopathology. Tumors were fixed in 4% formaldehyde and embedded in paraffin. Five µm sections were cut and imaged using the 700 nm and 800 nm channels of an Odyssey Infrared Imaging scanner (LI-COR). Images were generated at a resolution of 21 µm using two lasers, one emitting at 685 nm and the other at 785 nm. Consecutive sections were stained for cleaved caspase-3 (CC3), where a rabbit monoclonal anti-CC3 antibody (Cell Signaling Technology Inc,Danvers, MA) and a donkey anti-rabbit secondary biotinylated antibody (Jackson ImmunoResearch Laboratories. West Grove, PA) were used in a Polymer Refine Kit on an automated Bond platform (Leica Biosystems Ltd, Newcastle, UK); or they were stained using TdT-mediated dUTP Nick-End Labeling (TUNEL) using a DeadEnd Colorimetric system kit (Promega Benelux BV, Leiden, The Netherlands). Stained sections were scanned on an Aperio AT2 (Leica Biosystems) at x20 magnification, with a resolution of 0.5 µm per pixel. All annotations were performed with ImageScope (Leica Biosystems) and the stained surface area was quantified using the algorithm 'Positive Pixel Count v9' in Imagescope.

Statistical analysis. Statistical analyses were performed in GraphPad Prism (GraphPad Software, La Jolla, CA). Data are shown as mean ± standard deviation, unless stated otherwise. A two-tailed Student T-test was used for pairwise

comparisons. Pearson's r test was used to assess the significance of the correlation between CC3 staining and tumor binding of C2Am-750. P values of <0.05 were considered significant.

Results

HT-29 cells were largely resistant to MEDI3039, showing minimal loss of viability up to 10 pM drug concentration and only ~25% loss at much higher drug concentrations, whereas Colo205 cells showed ~50% loss of viability at low drug concentrations (EC50 1.3 pM) and complete loss of viability at higher drug concentrations (Figure 1A). This loss of viability, measured by Trypan blue dye exclusion, was mirrored in Colo-Dual cells by loss of bioluminescence (Figure 1B&C). Colo-Dual cells were transduced with a lentiviral vector to express firefly luciferase and the red fluorescent protein, mStrawberry. The bioluminescence signal from these cells is indicative of intracellular ATP concentration. Binding of C2Am labeled with a fluorescent dye excited at 750 nm (C2Am-750) and a site-directed mutant inactive in PS binding labeled with a fluorescent dye excited at 672nm (iC2Am-680) to MEDI3039-treated cells was characterized using confocal microscopy (Figure 2A) and flow cytometry (Figure 2B). The specificity of C2Am-750 for PS binding was confirmed by a blocking study with unlabeled C2Am (Supplementary Figure 1). Confocal microscopy measurements with Colo205-Dual cells treated with MEDI3039, showed that when compared to untreated cells there were relatively low levels of both NADH (intrinsic autofluorescence) and mStrawberry fluorescence, indicating cell death. These cells showed binding of C2Am-750 to the plasma membrane but negligible binding of iC2Am-680. There was negligible binding of C2Am-750 to untreated cells (Figure 2A). Flow cytometry of MEDI3039-treated TRAIL-sensitive Colo205 cells, but not

TRAIL-resistant HT-29 cells, showed increased binding of C2Am-750, which was correlated with a decrease in NADH autofluorescence and an increase in binding of a cell necrosis marker, Sytox Green (Figure 2B). iC2Am-680 showed negligible binding to either cell line, regardless of drug treatment.

Next, we investigated the capability of C2Am-750 to detect tumor cell death *in vivo*, in Colo205 and HT-29 xenografts in BALB/c *nu/nu* mice. Three hours after probe injection, there was a significant increase in C2Am-750 retention in treated as compared to untreated Colo205 tumors, which was observed both in fluorescence measurements made *in vivo* (5.97-fold, $P < 0.001$) and on excised tumors *ex vivo* (4.1-fold, P value < 0.001) (Figure 3). Compared to C2Am-750, the retention of iC2Am-680 was significantly lower in both treated ($P < 0.001$) and untreated ($P < 0.001$) tumors. These results were similar to those obtained previously with 5-fluorouracil (5-FU)-treated Colo205 tumors (250 mg/kg of body weight; injected intraperitoneally), in which C2Am and iC2Am, both labeled with AlexaFluor™-750 C5-maleimide, were injected separately (25). There was no significant difference in C2Am-750 retention in treated and untreated HT-29 xenografts, which was comparable to the retention observed in untreated Colo205 tumors (Supplementary Figure 2). iC2Am-680 retention was much lower in both groups. Fluorescence images of Colo205 tumor sections showed strong fluorescence signals from C2Am-750 (green) that co-localized with regions stained with TUNEL (a marker of necrotic cell death) and cleaved caspase 3 (CC3, a marker of apoptotic cell death). There was negligible signal from iC2Am-680 (blue), confirming the specificity of C2Am-750 for binding to dead and dying cells (Figure 3B). Measurements of bioluminescence from Colo-Dual tumors showed that at this single dose of MEDI3039 (0.4 mg/kg)

there was a complete loss of signal within 24 h of drug treatment, which was maintained for up to 45 days after treatment (Figure 4A). The rapid loss of bioluminescence in treated tumors, presumably due to loss of ATP (Figure 4B), preceded decreases in tumor volume, which started one week after treatment.

Next, we used MSOT to image retention of C2Am-750 and iC2Am-750 in MEDI3039-treated Colo205 tumors. The system used here had a spatial resolution of ~150 µm at a penetration depth of 3 cm. Spectral unmixing was used to generate images of C2Am-750, iC2Am-750 and intrinsic tissue chromophores (deoxygenated and oxygenated hemoglobin) throughout the entire tumor volume. Representative MSOT images show that there was some retention of C2Am-750 in untreated tumors (Figure 5A). However, signal from C2Am-750 was increased markedly at 7 h after drug treatment and 3 h after probe injection. Maximal signal from C2Am-750 appeared in the center of the treated tumors (Figure 5B), whereas there was negligible retention of iC2Am-750 (Figure 5C). Signal from kidney cortex confirmed that similar concentrations of C2Am-750 and iC2Am-750 had been injected in these animals. Axial, coronal and sagittal views showed that C2Am-750 was distributed throughout the entire tumor volume (Figure 5D). Images reconstructed in three dimensions are shown in Figure 5E (video representations of these images are in supplementary data). An MSOT absorption spectrum from a region of high signal intensity at the center of a MEDI3039-treated tumor obtained 3 h after injection of C2Am-750 was similar to the optical absorption spectrum of C2Am-750 measured *in vitro* (Supplementary Figure 3), demonstrating that the MSOT signal observed *in vivo* arose predominantly from C2Am-750.

Dynamic MSOT measurements with C2Am-750 and iC2Am-750 in MEDI3039-treated Colo205 tumors and parallel fluorescence images acquired from the same animals are shown in Figure 6. Both the MSOT (Figure 6A) and fluorescence images (Figure 6B) showed tumor retention of C2Am-750 for up to 24 h following probe injection, whereas there were only very low levels of iC2Am-750 in the tumor at 3 h and this had cleared by 24 h. At 24 h, the tumor signal-to-background ratio in animals injected with C2Am-750, in regions where there were high levels of C2Am-750 binding, increased from 1.3 ± 0.5 prior to probe injection to 15.0 ± 4.0 following probe injection (ratio ± S.E.M., n = 5), whereas this ratio did not change in animals injected with iC2Am-750 (Figure 6C). The average volume occupied by bound C2Am in drug-treated tumors at 24 h post probe injection was correlated with CC3 staining of tumor sections obtained post mortem, where the tumors were excised immediately following imaging (R^2=0.97, P value<0.01) (Figure 6D). Similar fluorescence signal intensities for C2Am-750 and iC2Am-750 were observed in the kidneys of these animals, confirming again that similar concentrations of the two probes had been injected.

We have shown previously that fluorescently labeled C2Am can detect cell death in EL4 murine lymphoma cells treated with etoposide and MDA-MB-231 human breast cancer cells treated with doxorubicin (5) and that C2Am labeled with fluorescent and radionuclide labels can detect cell death in etoposide-treated EL4 tumors, cyclophosphamide-treated Eμ-myc tumors and Colo205 tumors treated with 5-FU (25). Results of MSOT experiments with C2Am-750 in 5-FU-treated Colo-205 tumors are shown in Supplementary Figure 4. There was a significant increase in the MSOT signal from C2Am-750 at 24 h after 5-FU treatment and 3 h after probe

injection. A biodistribution study based on C2Am-750 fluorescence showed a significant increase in C2Am-750 retention in excised tumors compared to that in blood (4.05-fold, $P < 0.001$). Biodistribution data for fluorophore-labeled (i)C2Am-750 has been reported previously, where we showed that the biodistribution profiles were similar to those of ^{99m}Tc- and ^{111}In-labeled C2Am (25).

Discussion

Cell death, whether by apoptosis or necrosis, has attracted considerable attention as an imaging target since it is a generic marker for the presence of disease and additionally, in the case of cancer, a marker of response to treatment (4,29). A number of cell death imaging agents have been developed, with some interacting with intracellular targets, such as CC3 (30), cytosolic proteins (31,32) and the mitochondrial membrane potential (33); or with extracellular targets, including exposed extracellular DNA (34), histones (35) and plasma membrane phospholipids (6,36). Plasma membrane phospholipids, such as PS and phosphatidylethanolamine (PE), which are normally present on the inner leaflet of the plasma membrane bilayer, are exposed on the surface of apoptotic cells and in necrotic cells by permeabilization of the plasma membrane to the imaging agent (37,38). These phospholipids are an attractive target since in necrotic cells their exposure is persistent, which makes timing of imaging after cell death less critical, and they are abundant and therefore potentially capable of giving high signal-to-noise when bound by the imaging probe (7,39). In a previous study, titration of isolated apoptotic cells with fluorescently labeled C2Am gave an exposed PS concentration of 100 – 300 pmol/10^6 cells (5), which assuming a tumor cell density *in vivo* of ~10^8 cells/ml, corresponds to a PS concentration in apoptotic tumor tissue of 10 – 30 μM. This

concentration is considerably in excess of the estimated minimum MSOT-detectable dye concentration in mouse tissue of 0.5 – 2 μM (14).

We have shown previously that C2A, when conjugated to labels detectable by magnetic resonance (6,9), radionuclide and fluorescence imaging (25), is capable of detecting tumor cell death in vivo by binding to exposed PS. We have also shown that C2Am is more specific than Annexin V in detecting cell death, which also binds PS, since C2Am shows less binding to viable cells (5). The specificity of C2Am for detecting cell death was confirmed here by fluorescence measurements performed with C2Am and iC2Am *in vitro* and *in vivo* using MEDI3039-sensitive (Colo205) and resistant (HT-29) cell lines. Flow cytometry showed negligible binding of iC2Am and increased binding of C2Am to drug treated Colo205 cells but not to HT-29 cells. These findings were confirmed in implanted tumors *in vivo* and *ex vivo* by planar fluorescence imaging. Histological analysis of Colo205 tumor sections confirmed binding of C2Am-750 to apoptotic and necrotic cells.

Several targeted contrast agents for optoacoustic imaging of tumors have been developed in recent years (14,40,41), including dye-conjugated EGF, which was used to image EGF receptor expression in an orthotropic pancreatic cancer model (42), and a dye-conjugated cyclic peptide, which was used to image expression of the integrin, $\alpha_v\beta_3$, in an orthotropic brain tumor model (43). There has been a recent preliminary study in which a PS-binding antibody was used to image cell death in an implanted human breast cancer model in nude mice (44). However, the injected concentration was not specified nor was the statistical significance of the increase in signal intensity, which only appeared to be increased significantly at a time when the

tumor was already shrinking. Moreover, there was no histological validation, or control measurements with a non-PS binding IgG.

We have shown here that MSOT measurements with a NIR fluorophore-labeled PS binding protein, C2Am-750, can be used to create 3D images of tumor cell death in human colorectal xenografts treated with a novel TRAILR2 agonist, MEDI3039. The C2Am-750 signal in treated Colo205 tumors increased as early as 3 h post probe injection, and at 24 h the signal-to-background ratio, for those regions showing the greatest binding, was >10. There was negligible retention of a site-directed mutant of C2Am, which is inactive in PS binding (iC2Am-750) (Figure 6 A-C). Positive MSOT signal showed a good correlation with staining of apoptotic cells in tumor sections.

A limitation of the current study was the very high levels of tumor cell death following treatment with MEDI3039. However, we have shown previously that fluorescence imaging with C2Am labeled with AlexaFluor™-750 C5-maleimide was capable of detecting 5-FU-induced cell death in Colo205 tumors, where CC3 staining in tumor sections increased from 1 – 2% pre-treatment to 2 – 5% post treatment (25). Moreover, we have shown here that MSOT imaging with C2Am labeled with another NIR fluorophore was also capable of detecting 5-FU-induced tumor cell death. Tumor cell death in the clinic can range from less than 2% before treatment to 5%–15% after treatment (45).

Optoacoustic imaging with the C2Am probe described here has the potential to be used in the clinic to assess early treatment response in relatively superficial tumors,

such as in the breast (46), and in an endoscopic format (47), for assessing treatment response in tumors in the gastrointestinal tract.

Acknowledgements

We thank the CRUK Cambridge Institute Histopathology, Flow cytometry, Microscopy and Research Instrumentation Core Units, for their technical support and James Joseph, Neal Burton and Luis Santana for their advice on MSOT data analysis.

Author contributions

BX conducted all the experiments. MT supported the MSOT measurements. AAN designed the probe synthesis and purification protocols and contributed to data analysis. SR and BX made the Colo205-Dual cells. BX and SM prepared the labeled probes D-E H supported all the animal experiments, SRM, DT, RCAS and RWW provided advice on drug use and the appropriate tumor models, SEB advised on quantitation of the MSOT signals, KMB conceived the study and wrote the paper with BX. All authors reviewed the manuscript.

References

1. Dawson SJ, Tsui DW, Murtaza M, Biggs H, Rueda OM, Chin SF*, et al.* Analysis of circulating tumor DNA to monitor metastatic breast cancer. N Engl J Med **2013**;368(13):1199-209 doi 10.1056/NEJMoa1213261.
2. Zardavas D, Irrthum A, Swanton C, Piccart M. Clinical management of breast cancer heterogeneity. Nat Rev Clin Oncol **2015**;12(7):381-94 doi 10.1038/nrclinonc.2015.73.
3. Brindle K. New approaches for imaging tumour responses to treatment. Nat Rev Cancer **2008**;8(2):94-107 doi 10.1038/nrc2289.
4. Neves AA, Brindle KM. Imaging cell death. J Nucl Med **2014**;55(1):1-4 doi 10.2967/jnumed.112.114264.

5. Alam IS, Neves AA, Witney TH, Boren J, Brindle KM. Comparison of the C2A domain of synaptotagmin-I and annexin-V as probes for detecting cell death. Bioconjugate chemistry **2010**;21(5):884-91 doi 10.1021/bc9004415.
6. Zhao M, Beauregard DA, Loizou L, Davletov B, Brindle KM. Non-invasive detection of apoptosis using magnetic resonance imaging and a targeted contrast agent. Nat Med **2001**;7(11):1241-4 doi 10.1038/nm1101-1241 nm1101-1241 [pii].
7. Jung HI, Kettunen MI, Davletov B, Brindle KM. Detection of apoptosis using the C2A domain of synaptotagmin I. Bioconjugate chemistry **2004**;15(5):983-7 doi 10.1021/bc049899q.
8. Fang W, Wang F, Ji S, Zhu X, Meier HT, Hellman RS*, et al.* SPECT imaging of myocardial infarction using 99mTc-labeled C2A domain of synaptotagmin I in a porcine ischemia-reperfusion model. Nuclear medicine and biology **2007**;34(8):917-23 doi 10.1016/j.nucmedbio.2007.06.014.
9. Krishnan AS, Neves AA, de Backer MM, Hu DE, Davletov B, Kettunen MI*, et al.* Detection of cell death in tumors by using MR imaging and a gadolinium-based targeted contrast agent. Radiology **2008**;246(3):854-62 doi 10.1148/radiol.2463070471.
10. Blankenberg FG. In vivo detection of apoptosis. J Nucl Med **2008**;49 Suppl 2:81S-95S doi 10.2967/jnumed.107.045898.
11. Rice BW, Contag CH. The importance of being red. Nat Biotechnol **2009**;27(7):624-5 doi nbt0709-624 [pii] 10.1038/nbt0709-624.
12. Hong G, Antaris AL, Dai H. Near-infrared fluorophores for biomedical imaging. Nature Biomedical Engineering **2017**;1:0010 doi 10.1038/s41551-016-0010 http://www.nature.com/articles/s41551-016-0010 - supplementary-information.
13. Condeelis J, Weissleder R. In vivo imaging in cancer. Cold Spring Harb Perspect Biol **2010**;2(12):a003848 doi cshperspect.a003848 [pii] 10.1101/cshperspect.a003848.
14. Taruttis A, Ntziachristos V. Advances in real-time multispectral optoacoustic imaging and its applications. Nat Photon **2015**;9(4):219-27 doi 10.1038/nphoton.2015.29.
15. Dean-Ben XL, Fehm TF, Gostic M, Razansky D. Volumetric hand-held optoacoustic angiography as a tool for real-time screening of dense breast. J Biophotonics **2016**;9(3):253-9 doi 10.1002/jbio.201500008.
16. Heijblom M, Piras D, Xia W, van Hespen JC, Klaase JM, van den Engh FM*, et al.* Visualizing breast cancer using the Twente photoacoustic mammoscope: what do we learn from twelve new patient measurements? Opt Express **2012**;20(11):11582-97 doi 10.1364/OE.20.011582.
17. Manohar S, Vaartjes SE, van Hespen JCG, Klaase JM, van den Engh FM, Steenbergen W*, et al.* Initial results of in vivo non-invasive cancer imaging in the human breast using near-infrared photoacoustics. Optics Express **2007**;15(19):12277-85 doi 10.1364/oe.15.012277.
18. Stoffels I, Morscher S, Helfrich I, Hillen U, Leyh J, Burton NC*, et al.* Metastatic status of sentinel lymph nodes in melanoma determined noninvasively with multispectral optoacoustic imaging. Sci Transl Med **2015**;7(317):317ra199 doi 10.1126/scitranslmed.aad1278.
19. Waldner MJ, Knieling F, Egger C, Morscher S, Claussen J, Vetter M*, et al.* Multispectral Optoacoustic Tomography in Crohn's Disease: Noninvasive

Imaging of Disease Activity. Gastroenterology **2016**;151(2):238-40 doi 10.1053/j.gastro.2016.05.047.
20. Johnstone RW, Frew AJ, Smyth MJ. The TRAIL apoptotic pathway in cancer onset, progression and therapy. Nat Rev Cancer **2008**;8(10):782-98 doi 10.1038/nrc2465.
21. Prasad S, Kim JH, Gupta SC, Aggarwal BB. Targeting death receptors for TRAIL by agents designed by Mother Nature. Trends in pharmacological sciences **2014**;35(10):520-36 doi 10.1016/j.tips.2014.07.004.
22. Tuthill MH, Montinaro A, Zinngrebe J, Prieske K, Draber P, Prieske S*, et al.* TRAIL-R2-specific antibodies and recombinant TRAIL can synergise to kill cancer cells. Oncogene **2015**;34(16):2138-44 doi 10.1038/onc.2014.156.
23. Greer YE, Tice D, Lipkowitz S. MEDI3039, a novel highly potent tumor necrosis factor (TNF)-related apoptosis inducing ligand (TRAIL) receptor agonist, induces apoptotic cell death in breast cancer cells. Cancer Research **2016**;76 doi 10.1158/1538-7445.sabcs15-p5-03-06.
24. Swers JS, Grinberg L, Wang L, Feng H, Lekstrom K, Carrasco R*, et al.* Multivalent scaffold proteins as superagonists of TRAIL receptor 2-induced apoptosis. Molecular cancer therapeutics **2013**;12(7):1235-44 doi 10.1158/1535-7163.MCT-12-1107.
25. Neves AA, Xie B, Fawcett S, Alam IS, Witney TH, de Backer MM*, et al.* Rapid Imaging of Tumor Cell Death In Vivo Using the C2A Domain of Synaptotagmin-I. J Nucl Med **2017**;58(6):881-7 doi 10.2967/jnumed.116.183004.
26. Patrick PS, Hammersley J, Loizou L, Kettunen MI, Rodrigues TB, Hu DE*, et al.* Dual-modality gene reporter for in vivo imaging. Proc Natl Acad Sci U S A **2014**;111(1):415-20 doi 10.1073/pnas.1319000111.
27. Dima A, Burton NC, Ntziachristos V. Multispectral optoacoustic tomography at 64, 128, and 256 channels. J Biomed Opt **2014**;19(3):36021 doi 10.1117/1.JBO.19.3.036021.
28. Razansky D, Buehler A, Ntziachristos V. Volumetric real-time multispectral optoacoustic tomography of biomarkers. Nat Protoc **2011**;6(8):1121-9 doi nprot.2011.351 [pii]
10.1038/nprot.2011.351.
29. Smith BA, Smith BD. Biomarkers and molecular probes for cell death imaging and targeted therapeutics. Bioconjugate chemistry **2012**;23(10):1989-2006 doi 10.1021/bc3003309.
30. Barnett EM, Zhang X, Maxwell D, Chang Q, Piwnica-Worms D. Single-cell imaging of retinal ganglion cell apoptosis with a cell-penetrating, activatable peptide probe in an in vivo glaucoma model. Proc Natl Acad Sci U S A **2009**;106(23):9391-6 doi 0812884106 [pii]
10.1073/pnas.0812884106.
31. Park D, Don AS, Massamiri T, Karwa A, Warner B, MacDonald J*, et al.* Noninvasive imaging of cell death using an Hsp90 ligand. J Am Chem Soc **2011**;133(9):2832-5 doi 10.1021/ja110226y.
32. Xie B, Stammes MA, van Driel PB, Cruz LJ, Knol-Blankevoort VT, Lowik MA*, et al.* Necrosis avid near infrared fluorescent cyanines for imaging cell death and their use to monitor therapeutic efficacy in mouse tumor models. Oncotarget **2015** doi 10.18632/oncotarget.5498.
33. Reshef A, Shirvan A, Shohami E, Grimberg H, Levin G, Cohen A*, et al.* Targeting cell death in vivo in experimental traumatic brain injury by a novel

molecular probe. J Neurotrauma **2008**;25(6):569-80 doi 10.1089/neu.2007.0341.
34. Dasari M, Lee S, Sy J, Kim D, Brown M, Davis M*, et al.* Hoechst-IR: an imaging agent that detects necrotic tissue in vivo by binding extracellular DNA. Org Lett **2010**;12(15):3300-3 doi 10.1021/ol100923d.
35. Wang K, Purushotham S, Lee JY, Na MH, Park H, Oh SJ*, et al.* In vivo imaging of tumor apoptosis using histone H1-targeting peptide. J Control Release **2010**;148(3):283-91 doi S0168-3659(10)00753-4 [pii] 10.1016/j.jconrel.2010.09.010.
36. Zhao M, Li Z, Bugenhagen S. 99mTc-labeled duramycin as a novel phosphatidylethanolamine-binding molecular probe. J Nucl Med **2008**;49(8):1345-52 doi 10.2967/jnumed.107.048603.
37. Majno G, Joris I. Apoptosis, oncosis, and necrosis. An overview of cell death. Am J Pathol **1995**;146(1):3-15.
38. Martin SJ, Reutelingsperger CP, McGahon AJ, Rader JA, van Schie RC, LaFace DM*, et al.* Early redistribution of plasma membrane phosphatidylserine is a general feature of apoptosis regardless of the initiating stimulus: inhibition by overexpression of Bcl-2 and Abl. J Exp Med **1995**;182(5):1545-56.
39. Elvas F, Vangestel C, Rapic S, Verhaeghe J, Gray B, Pak K*, et al.* Characterization of [(99m)Tc]Duramycin as a SPECT Imaging Agent for Early Assessment of Tumor Apoptosis. Molecular imaging and biology : MIB : the official publication of the Academy of Molecular Imaging **2015**;17(6):838-47 doi 10.1007/s11307-015-0852-6.
40. McNally LR, Mezera M, Morgan DE, Frederick PJ, Yang ES, Eltoum IE*, et al.* Current and Emerging Clinical Applications of Multispectral Optoacoustic Tomography (MSOT) in Oncology. Clin Cancer Res **2016**;22(14):3432-9 doi 10.1158/1078-0432.CCR-16-0573.
41. Weber J, Beard PC, Bohndiek SE. Contrast agents for molecular photoacoustic imaging. Nat Methods **2016**;13(8):639-50 doi 10.1038/nmeth.3929.
42. Hudson SV, Huang JS, Yin W, Albeituni S, Rush J, Khanal A*, et al.* Targeted noninvasive imaging of EGFR-expressing orthotopic pancreatic cancer using multispectral optoacoustic tomography. Cancer Res **2014**;74(21):6271-9 doi 10.1158/0008-5472.CAN-14-1656.
43. Li ML, Oh JT, Xie XY, Ku G, Wang W, Li C*, et al.* Simultaneous molecular and hypoxia imaging of brain tumors in vivo using spectroscopic photoacoustic tomography. Proceedings of the IEEE **2008**;96(3):481-9 doi 10.1109/jproc.2007.913515.
44. Kannadorai RK, Udumala SK, Sidney YW. Noninvasive in vivo multispectral optoacoustic imaging of apoptosis in triple negative breast cancer using indocyanine green conjugated phosphatidylserine monoclonal antibody. J Biomed Opt **2016**;21(12):126002 doi 10.1117/1.JBO.21.12.126002.
45. Nguyen Q-D, Smith G, Glaser M, Perumal M, Årstad E, Aboagye EO. Positron emission tomography imaging of drug-induced tumor apoptosis with a caspase-3/7 specific [(18)F]-labeled isatin sulfonamide. Proceedings of the National Academy of Sciences of the United States of America **2009**;106(38):16375-80 doi 10.1073/pnas.0901310106.

46. Kruger RA, Kuzmiak CM, Lam RB, Reinecke DR, Del Rio SP, Steed D. Dedicated 3D photoacoustic breast imaging. Med Phys **2013**;40(11):113301 doi 10.1118/1.4824317.
47. Yang JM, Favazza C, Chen R, Yao J, Cai X, Maslov K*, et al.* Simultaneous functional photoacoustic and ultrasonic endoscopy of internal organs in vivo. Nat Med **2012**;18(8):1297-302 doi 10.1038/nm.2823.

Figure legends

Figure 1. Differential sensitivity of Colo205 and HT-29 cells to TRAILR2 agonist-induced cell death. A. Dose response of Colo205 and HT-29 cells to MEDI3039. Cell viabilities were measured by Trypan blue dye exclusion after incubating the cells with various drug concentrations (0-400 pM) for 22 h. B. Dose response of Colo205-Dual cells, which express firefly luciferase, to MEDI3039. Loss of ATP in these cells results in a loss of bioluminescence. Cells were incubated with various drug concentrations (0-100 pM) for 22 h. C. Representative bioluminescence images of Colo205-Dual cells at 22 h after incubation with the indicated drug concentration. All experiments were performed in triplicate.

Figure 2. Detection of TRAILR2 agonist-induced cell death using C2Am. (**A**) Confocal microscopy of drug-treated (upper panel) and untreated (lower panel) Colo-Dual cells. Cell death was induced by treatment with 10 pM MEDI3039 for 5 h. The cells were co-incubated subsequently with C2Am-750 (green) and iC2Am-680 (red), washed and then imaged. Decreases in NADH autofluorescence (blue) and mStrawberry fluorescence (magenta) in treated cells indicated dead or dying cells. Merged images show the overlay of all the channels except the bright-field view. Scale bar = 5 µm. (**B**) Detection of drug-induced cell death in Colo205 and HT-29 cells using flow cytometry. Cells were untreated or treated with 1 pM MEDI3039 for 22 h and incubated subsequently with a cell necrosis marker, Sytox Green (upper panels), C2Am-750 (middle panels) or iC2Am-680 (lower panels). Low levels of NADH autofluorescence (x axis) and staining with Sytox Green were used to identify

dead cells. The numbers in the scatter plots represent the percentage of cells in the respective quadrants.

Figure 3. Fluorescence imaging of TRAILR2 agonist-induced tumor cell death *in vivo* and *ex vivo*. (**A**) Nude mice bearing subcutaneous Colo205 tumors were treated with a single dose of 0.4 mg/kg MED3039. Untreated mice were injected with solvent vehicle (PBS). After 16 h, the mice were injected with a mixture of 0.1 µmole/kg C2Am-750 and 0.1 µmole/kg iC2Am-680 followed by whole body FLI measurements using an IVIS 200 camera at 30 min and 3 h post probe injection. The white arrows indicate the location of the tumor. (**B**) Histological validation of C2Am-750 labeling of MEDI3039-induced tumor cell death. MEDI3039-treated and untreated Colo205 tumors were excised at 3 h post probe injection. Paraffin embedded tumor sections were scanned for fluorescence (green: C2Am-750; blue: iC2Am-680; signal intensity bars are shown on the right hand side) followed by TUNEL staining and staining for cleaved capase-3 (CC3). (**C**) Quantitation of *in vivo* tumor fluorescence intensities at 3 h post injection of C2Am-750 and iC2Am-680. (**D**) Quantitation of fluorescence intensities in excised tumors from animals injected with C2Am-750 and iC2Am-680. The intensities have been normalized to tumor weight. * P<0.05, ** P<0.01, ***p<0.001. Scale bar = 3 mm.

Figure 4. A single dose of TRAILR2 agonist produced a durable response in Colo-Dual tumors. (**A**) Colo-Dual cells (5×10^6) were implanted subcutaneously in nude mice at day 0. Bioluminescence measurements were made on the resulting tumors starting from day 11 when, in the treated group (n=5), animals were injected with a single dose of 0.4mg/kg MEDI3039. Untreated animals (n=5) were injected

with drug vehicle (PBS). (**B**) Representative bioluminescence images of treated and untreated mice on day 11 and day 12. Imaging measurements were made just before injection of MEDI3039 on day 11 and then 24 h later on day 12.

Figure 5. MSOT of treated and untreated mice injected with C2Am-750 or iC2Am-750. Nude mice bearing subcutaneous Colo205 tumors were either untreated (**A**) or treated with a single dose of 0.4 mg/kg MED3039 (**B&C**). At 4 h after drug treatment MSOT measurements were made before (left panels) and at 3 h post injection of 0.2 µmole/kg of (i)C2Am-750 (right panels). Signals from C2Am-750/iC2Am-750, oxygenated hemoglobin (HbO_2), deoxygenated hemoglobin (Hb) are shown in green, red and blue respectively. The tumor is outlined by a white line in a - c. (**D**) Representative axial, coronal and sagittal views of a tumor before and 3 h after injection of C2Am-750. (**E**) Representative 3D image of a tumor before and 3 h after injection of C2Am-750. Scale bar = 3 mm.

Figure 6. Serial measurements of C2Am-750 and iC2Am-750 retention in TRAILR2 agonist-treated Colo205 tumors. (**A**) Representative MSOT images of tumors (outlined), 4 h after drug treatment (0.4 mg/kg MED3039) and at the indicated times after injection of the probes. (**B**) Representative epi-fluorescence images acquired at the indicated times after probe injection. Signal was observed from the tumors (arrowed) and kidneys. (**C**) Quantification of probe uptake in 3D reconstructed volumes of interest (VOIs) in MSOT images acquired 24 h after probe injection. Signal-to-background ratios were calculated by dividing the mean pixel intensity (MPI) in a VOI within the tumor, where maximum signal was observed, by the MPI of an adjacent size-matched VOI. *** $P<0.001$ ($n = 5$) (**D**). Correlation of the

volume of tumor with bound C2Am-750 (VT), expressed as a percentage of the total tumor volume (T), with CC3 positive staining in non-consecutive tumor sections (five tumors; four sections per tumor). Scale bar = 3 mm.

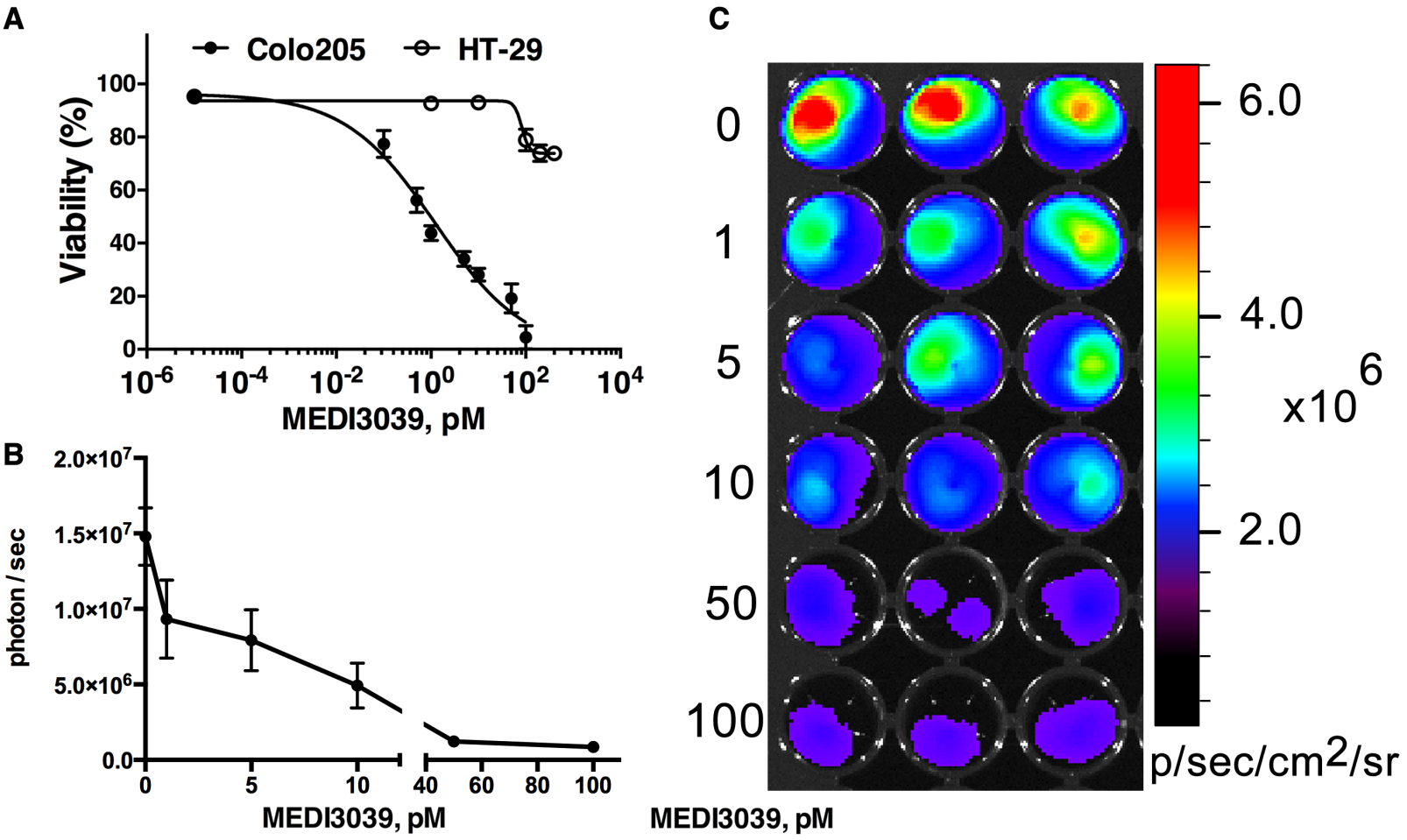
A
Colo205
HT-29
Viability (%)
100
80
60
40
20
0
10-6
10-4
10-2
100
102
104
MEDI3039, pM
B
photon / sec
2.0×107
1.5×107
1.0×107
5.0×106
0.0
0
5
10
40
60
80
100
MEDI3039, pM
C
0
1
5
10
50
100
6.0
4.0
2.0
x10 6
p/sec/cm2/sr
MEDI3039, pM

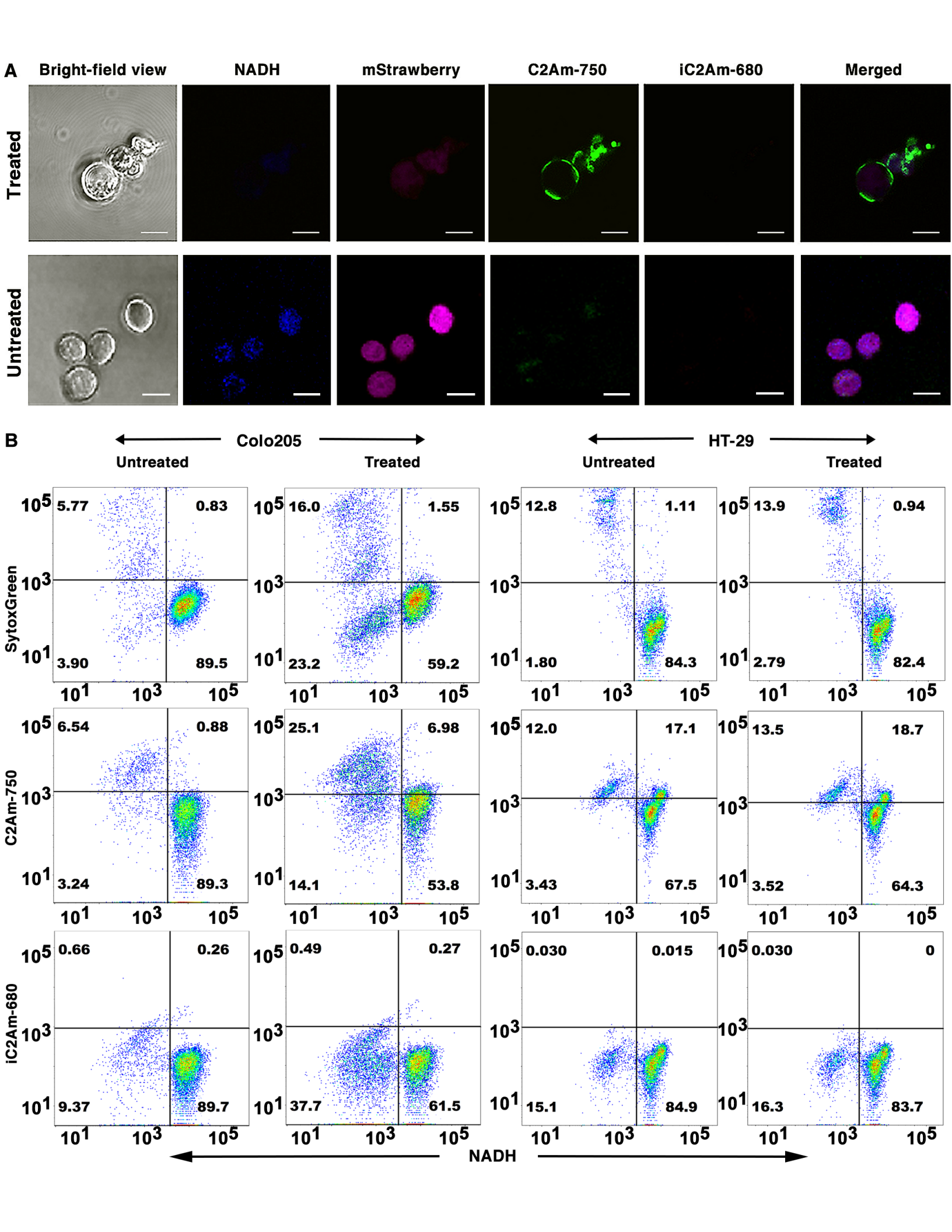
A
Bright-field view
NADH
mStrawberry
C2Am-750
iC2Am-680
Merged
Treated
Untreated
B
Colo205
HT-29
Untreated
Treated
Untreated
Treated
SytoxGreen
C2Am-750
iC2Am-680
5.77
0.83
3.90
89.5
16.0
1.55
23.2
59.2
12.8
1.11
1.80
84.3
13.9
0.94
2.79
82.4
6.54
0.88
3.24
89.3
25.1
6.98
14.1
53.8
12.0
17.1
3.43
67.5
13.5
18.7
3.52
64.3
0.66
0.26
9.37
89.7
0.49
0.27
37.7
61.5
0.030
0.015
15.1
84.9
0.030
0
16.3
83.7
NADH

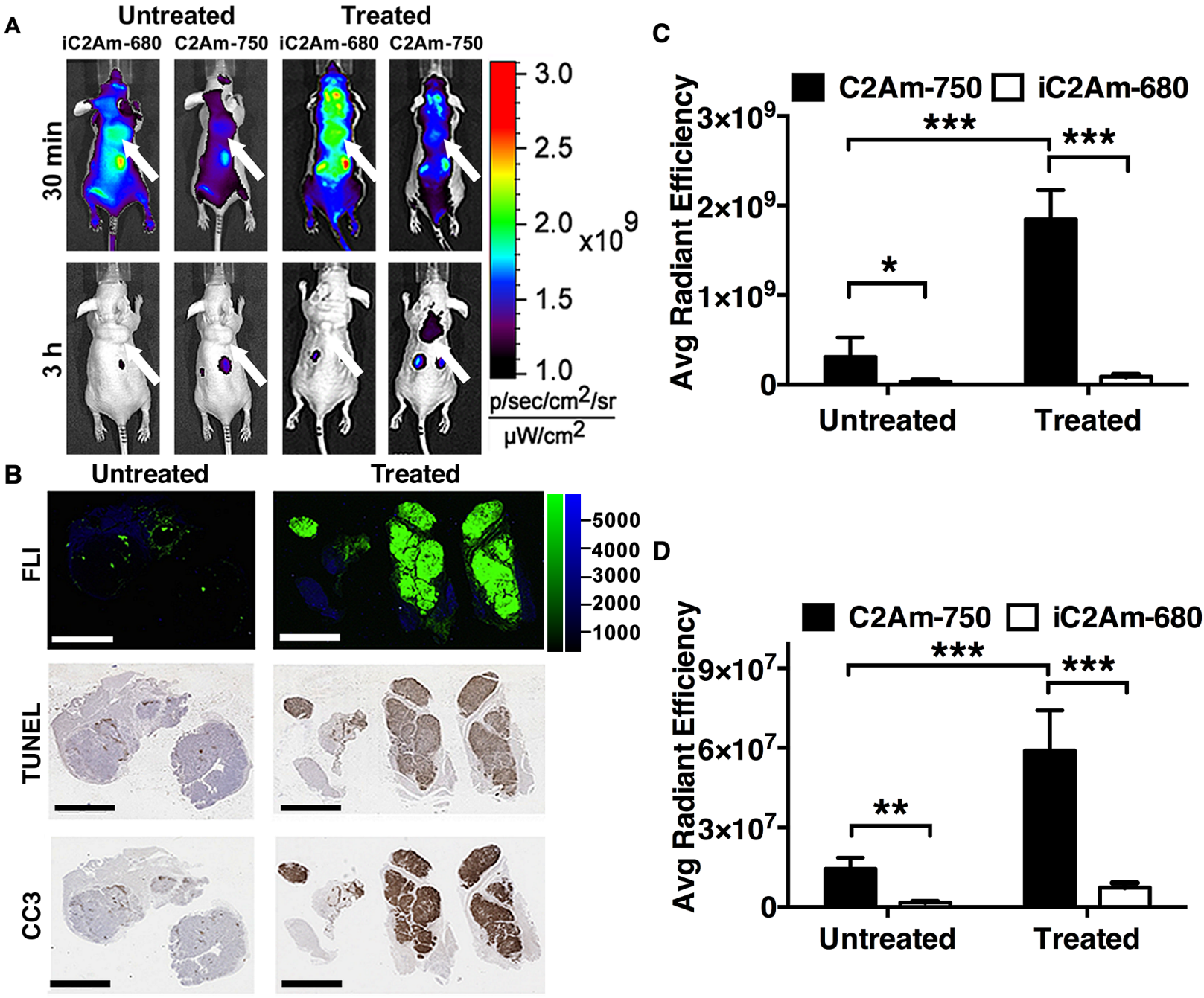
A
Untreated
Treated
iC2Am-680
C2Am-750
iC2Am-680
C2Am-750
30 min
3 h
3.0
2.5
2.0
1.5
1.0
x10^9
p/sec/cm2/sr
µW/cm2
B
Untreated
Treated
FLI
5000
4000
3000
2000
1000
TUNEL
CC3
C
C2Am-750
iC2Am-680
Avg Radiant Efficiency
3×10^9
2×10^9
1×10^9
0
***
***
*
Untreated
Treated
D
C2Am-750
iC2Am-680
Avg Radiant Efficiency
9×10^7
6×10^7
3×10^7
0
***
***
**
Untreated
Treated

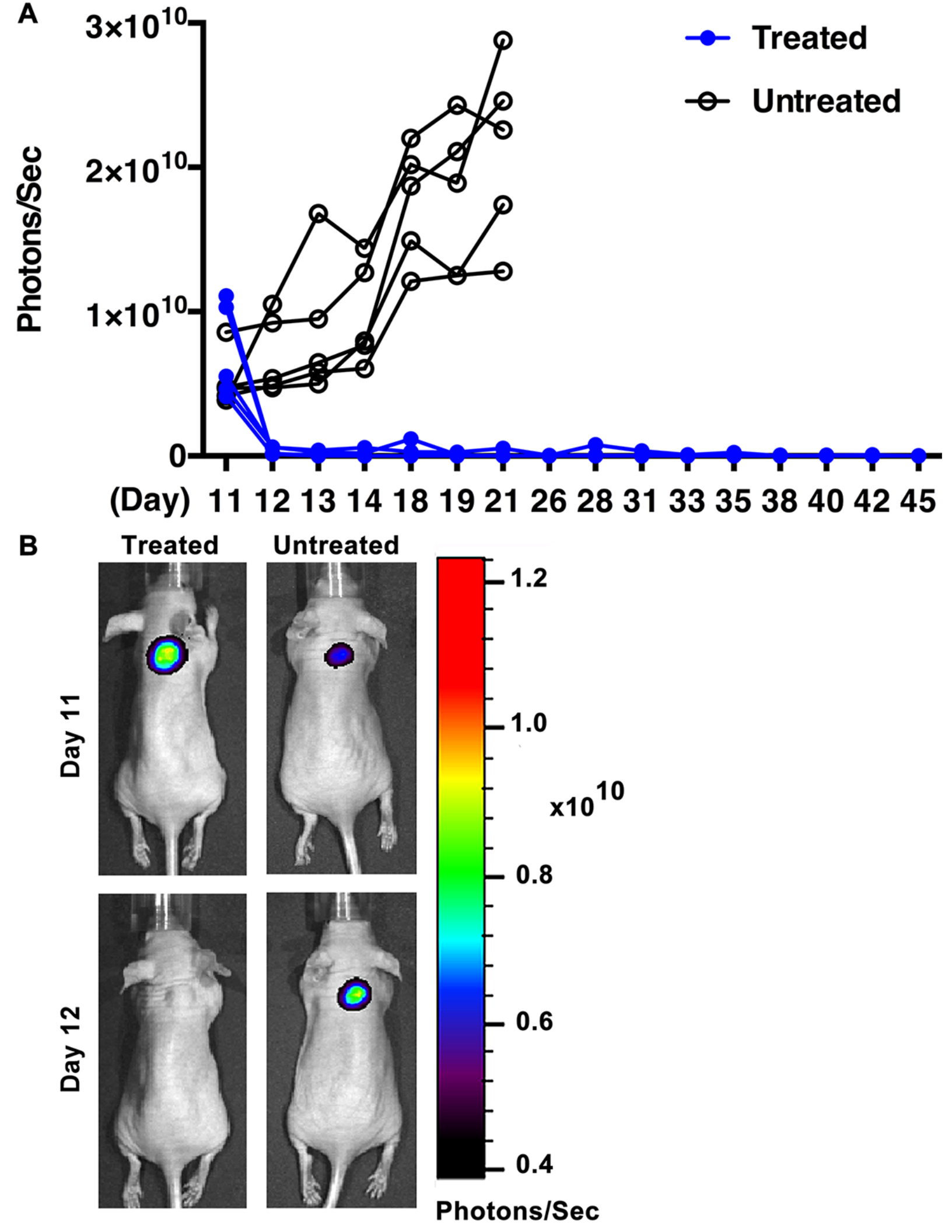
A
3×10^10
2×10^10
1×10^10
0
Photons/Sec
Treated
Untreated
(Day) 11 12 13 14 18 19 21 26 28 31 33 35 38 40 42 45
B
Treated
Untreated
Day 11
Day 12
1.2
1.0
0.8
0.6
0.4
x10^10
Photons/Sec

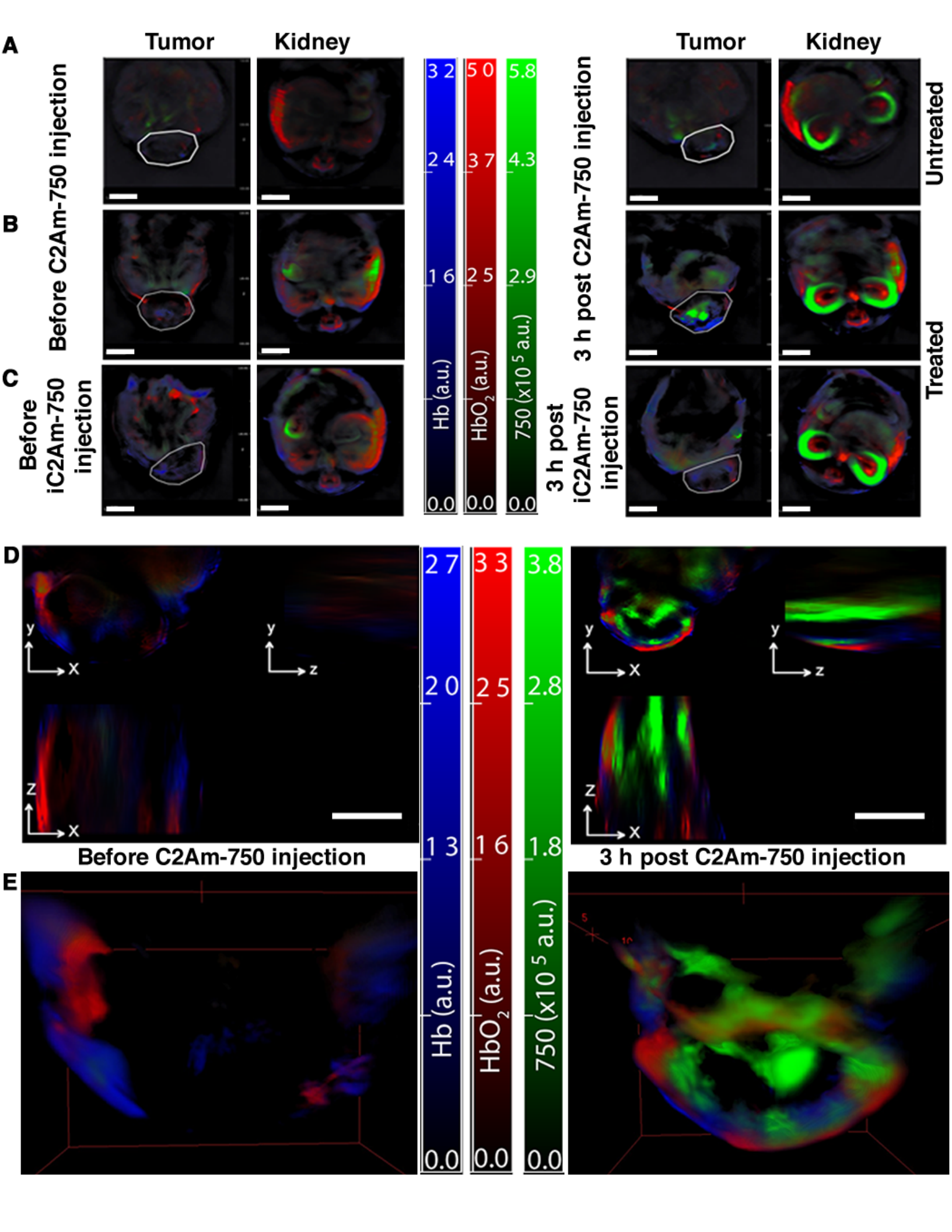
A
B
C
D
E
Tumor
Kidney
Before C2Am-750 injection
Before iC2Am-750 injection
3 h post C2Am-750 injection
3 h post iC2Am-750 injection
Untreated
Treated
3 2
2 4
1 6
0.0
Hb (a.u.)
5 0
3 7
2 5
0.0
HbO2 (a.u.)
5.8
4.3
2.9
0.0
750 (x10 5 a.u.)
2 7
2 0
1 3
0.0
Hb (a.u.)
3 3
2 5
1 6
0.0
HbO2 (a.u.)
3.8
2.8
1.8
0.0
750 (x10 5 a.u.)
Before C2Am-750 injection
3 h post C2Am-750 injection

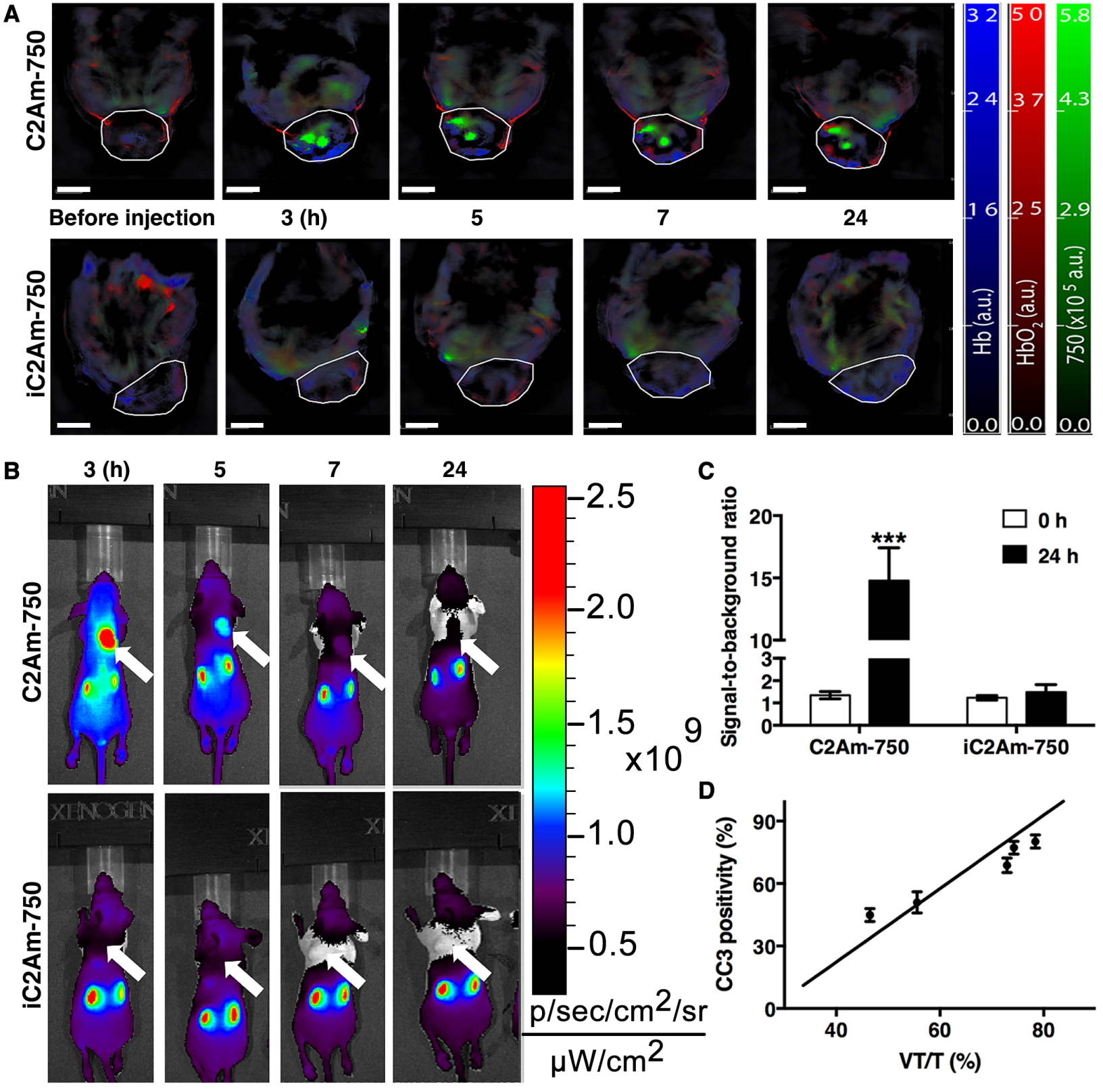
A
C2Am-750
iC2Am-750
Before injection
3 (h)
5
7
24
3 2
2 4
1 6
0.0
Hb (a.u.)
5 0
3 7
2 5
0.0
HbO2 (a.u.)
5.8
4.3
2.9
0.0
750 (x10 5 a.u.)
B
3 (h)
5
7
24
C2Am-750
iC2Am-750
2.5
2.0
1.5
1.0
0.5
x10 9
p/sec/cm2/sr
µW/cm2
C
Signal-to-background ratio
0 h
24 h
***
C2Am-750
iC2Am-750
D
CC3 positivity (%)
VT/T (%)